Reply to Review 2

"In this manuscript, the authors evaluate the SW-domain properties of Arctic cirrus clouds as simulated by the IFS model by comparing them with airborne measurements. A similar study was recently published in ACP but for low-level clouds. The subject is important and useful. The work is of very good quality, the results are clear, the analyses relevant and the writing pleasant. This manuscript deserves to be published in ACP and only minor comments and suggestions are made below."

Thank you very much for this positive review of our paper. Before we address your comments and suggestions below, we would like to mention a few changes in the revised manuscript.

- In previous simulations using the VarCloud data as input we did not replace the cloud fraction from the IFS. We have now included this replacement and updated the solar transmissivity in the text as well as in the revised Fig 9.
- In the original version of Fig. 3 the abscissa axis in panel (d) was reversed, which it should not since RF 18 featured a circular flight pattern. We corrected this and the data is now displayed at the correct location.
- Figure 4: A new version of the dropsonde data set became available since submission of the manuscript. We updated Fig. 4 with this revised data set. The main difference is the removal of the NAN values visible in the previous relative humidity plots (panels (b) and (d)) and the removal of data above 10 km altitude, which is due to the interpolation of the data onto a uniform altitude grid.
- Due to comments from reviewer 1, we split the former Sect. 4 into two new sections with the revised Sect. 4 focusing on the comparison between the IFS forecast and the measured macrophysical properties of the cirrus (formerly Sect. 4.1), while the revised Sect. 5 includes a new subsection 5.2 focusing on the r_{eff} parameterization.
- Further, we moved the sea ice albedo section (formerly Sect. 4.2.3) to Sect. 5.1 to follow the same structure as in Sect. 3, where we also start with the sea ice albedo. The results of this experiment are also added to Table 3 showing the mean solar transmissivity of all conducted experiments. Due to this change in structure, we also moved the explanation of the calculation of the solar transmissivity into Sect. 5.1.

We also polished the text in the Abstract, the Introduction and the Summary and Conclusions. The rest of the reply is structured as follows, we first repeat your comment in blue italics and then reply to it. Please note that the line numbers in your comments are unchanged and still refer to the old version of the manuscript. We then quote the introduced changes in italics giving the line numbers in the revised manuscript. The revised figures can be found at the end of the reply. Within the reply we use the same abbreviations as in the manuscript, namely

- HALO (High Altitude LOng range research aircraft)
- IFS (Integrated Forecasting System)
- r_{eff} (ice effective radius)
- IWC (ice water content)
- IWP (ice water path)
- VarCloud (referring to the VarCloud microphysical retrieval from Ewald et al. (2021))
- ecRad (referring to the radiative transfer scheme (Hogan and Bozzo 2018))
- Fu-IFS, Yi2013 and Baran2016 (referring to the ice optics parameterization from Fu (1996), Yi et al. (2013) and Baran et al. (2016), respectively)

Comments

"1. l. 273-274: (comment on Fig. 4) If I understand correctly, the measurements shown between 11 and 11:30 correspond to the results of the simulation at 11:00, and the cloud evolution between 11 and 11:30 is

due to the displacement of the aircraft (i.e. the spatial evolution of the clouds) and not to the evolution of the clouds over time. I think this should mentioned more explicitly."

This is indeed correct. The distance HALO flies within 30 min and the covered spatial changes are more substantial than the temporal evolution of the cloud within these 30 min. This is investigated with Fig. 5 showing the IWC distributions for the 11 UTC and 12 UTC time step of the IFS. Apart from a small shift towards smaller values in RF 17 no substantial changes are observed between the two time steps. We adjusted a sentence and added one to clarify this.

L276-278: Added *"along the flight track of HALO."* to *"Figure 4 shows the VarCloud lidar-radar cloud mask from HALO, the aircraft altitude, and the predicted cloud fraction of the IFS along the flight track of HALO."*

L293: Added *"Thus, the change in cloud fraction shown here is mostly due to HALO flying through different grid cells."*

"2. l. 291-292: What do you mean by compensate? The effect of the cosine of the zenith angle?"

The solar zenith angle is quite large for both of our case studies. Especially for RF 17, flying westward, it also changes by about 2°, which amounts to about 25 W m^{-2} decrease of downward solar irradiance at the top of atmosphere. Thus, the transmitted solar downward irradiance below the cloud is dominated by this change in solar zenith angle. Analyzing the downward irradiance only, makes it harder to interpret other effects such as the inhomogeneity of the cirrus. Thus, we opted for the transmissivity as a relative measure, which partly compensates for changes of the solar zenith angle in our measurements. We rephrased the introductory sentence regarding the solar transmissivity to make this more clear.

L324-L325: Rephrased to *"The solar transmissivity, as a relative measure, thereby mostly compensates for the effect of the solar zenith angle, which would otherwise dominate the measurement."*

"3. Figure 8: What is the value of IWC to differentiate between clear and cloudy skies? How are the histograms modified for small values of IWC when this threshold is changed?"

This is a good question, with a not so easy answer as the IFS cloud fraction is a prognostic variable itself. Meaning there is no fixed threshold of IWC from which a cloud is diagnosed. It is more so that either there is a cloud fraction value predicted or not. This also allows for precipitating ice in cloud free grid cells. The values shown in now Fig. 9 are filtered and scaled with the IFS cloud fraction, thus representing only the in-cloud IWC. This is consistent with ecRad's treatment of clouds. ecRad only calculates ice optical properties for grid cells which are cloudy (cloud fraction > 0) and have an IWC greater 10^{-9} kg kg^{-1}. All the IWC values in our case studies are above this value. Because of this and since there is no IWC threshold to differentiate between clear and cloudy skies, the sensitivity of the small value bins in the histogram cannot be explored.

"4. l. 318-355 and Figure 9: The value of the IWC has an impact on the radiative flux and it is interesting to show the comparison between the measured values and those of the model. But the flux also depends on the vertical integral of the IWC (i.e. the ice water path, IWP). The IWP depends not only on the IWC but also on the way in which vertical overlaps occur. It would therefore be interesting to compare the IWP as well.

This is a good suggestion, which lead us to include the IWP in Sect. 5.4 "IWC and r_{eff} input", where we switch the IFS IWC and r_{eff} for the VarCloud retrieved values. Therefore, we added another row to now Fig. 9 showing the IWP distribution for the two case studies and adjusted the figure caption accordingly. We also adjusted the introduction of Fig. 9 and added an explanation of what can be seen in the IWP distributions.

Figure 9: Added two new panels (c) and (d) showing the IWP distributions from the IFS and VarCloud for the case study areas in RF 17 and RF 18, respectively.

L384-385: Rephrased to *"Due to the temporal resolution of VarCloud, more points are available for the retrieval compared to the IFS while the IWP distributions naturally have less data points."*

L389-L396: Added *"For RF 17 only very low IWP values below* $20\,g\,m^{-2}$ *are observed in the VarCloud data, while the IFS also shows values up to* $80\,g\,m^{-2}$*. Nonetheless, most of the IFS values are also concentrated in the first two bins below* $20\,g\,m^{-2}$ *giving both distributions a strong positive skewness. This shows that, although the IFS predicts more smaller IWC values during RF 17, it overpredicts the IWP and thus the optical thickness as has already been shown with the solar transmissivity in Fig. 7. The histograms for RF 18 in Fig. 9 (d), in analogy to the IWC distributions, are flatter and show more large values. Apart from the VarCloud data showing more values in the lower bins between* $20\,g\,m^{-2}$ *and* $40\,g\,m^{-2}$ *and the IFS data having values above* $90\,g\,m^{-2}$*, which the VarCloud data is missing, the distributions are rather similar."*

"5. l. 390-391: You talk about the effect of 'reice' on the model results, but what is the sensitivity of the estimated values to r_{eff}*? Are the values of* r_{eff} *used consistent with those of the model?"*

We assume, the first question addresses the similar analysis of the parameterization of r_{eff} as recommended by reviewer 1. We added a paragraph with a sensitivity study at the beginning of Sect. 5.2 concerning the r_{eff} parameterization. With this we could show that by varying r_{eff} in its allowed range, changes of the solar downward irradiance below cloud between $-5\,\%$ and $+35\,\%$ are possible.

L347-L352: *To explore the sensitivity of the ecRad simulations to* r_{eff} *the* 12 *UTC time step from the below cloud section of RF 18 is taken and* r_{eff} *inside the cloud is varied in the possible range of values between* $13\,\mu m$ *and* $100\,\mu m$*. The simulations are preformed using the reference setup with the IFS IWC and the Fu-IFS ice optics parameterization. Comparing the solar downward irradiance below the cloud across all simulations shows a change between* $-5\,\%$ *to* $+35\,\%$ *with respect to the original value. Thus, we conclude that* r_{eff} *is indeed one of the driving factors in the ecRad simulations.*

We are not quite sure, what the second part of your question refers to. It could mean, whether the VarCloud retrieved r_{eff} values are within the range of the possible values predicted by the Sun (2001) parameterization. If that is the case, the question can be answered with a yes. The maximum value returned by Sun (2001) within the IFS is $100\,\mu\mathrm{m}$ and all retrieved values are below that. The Sun (2001) parameterization could theoretically return larger values, but the implementation within the IFS caps the maximum value, because the ice optics parameterization by Fu (1996) would result in asymmetry parameters larger than 1 for r_{eff} larger than $100\,\mu\mathrm{m}$.

Another interpretation of your question could concern the difference in definition of r_{eff} between the Sun and Rikus (1999) parameterization and the VarCloud retrieval by Ewald et al. (2021). Both r_{eff} definitions are either taken directly from Foot (1988) (VarCloud) or can be related to it (Sun and Rikus 1999). However, while Sun and Rikus (1999) assume hexagonal columns as a particle shape, Ewald et al. (2021) use the horizontally aligned oblate spheroid approximation from Hogan et al. (2012). This is due to the two papers trying to achieve quite different objectives. Ewald et al. (2021) want to retrieve microphysical properties from active remote sensing measurements and thus need to simulate radar and lidar signals, from which they then derive the IWC and r_{eff}. Sun and Rikus (1999) on the other hand want to use the IWC and temperature predicted by a model as input to parameterize r_{eff}. The parameterized r_{eff} can then be used in ice optics parameterization.

Hopefully, one of the two explanations answered your question.

Revised figures

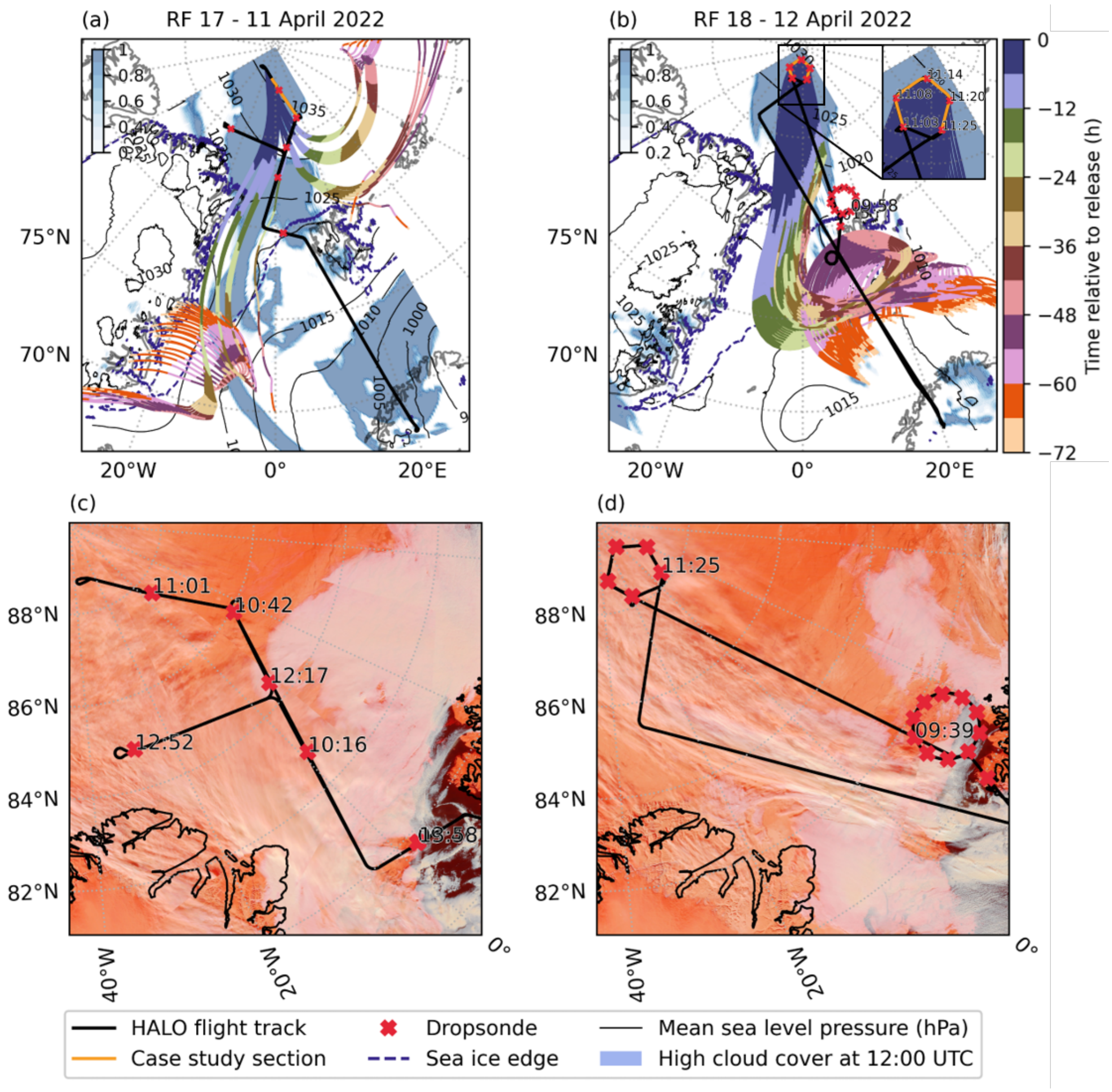

Figure 1: Map of flight tracks with IFS predicted high cloud cover for 12 UTC, sea ice edge (80 % sea ice cover), mean sea level pressure isolines, dropsonde locations (red crosses), highlighted case study regions (orange), and LAGRANTO backward trajectories for (a) RF 17 and (b) RF 18. The box in panel (b) shows a zoom of the case study region with the above and below-cloud flight sections for RF 18. (c) and (d) False color corrected reflectance from MODIS on Terra using Band 3, 6 and 7 for RF 17 and RF 18, respectively, as provided by the Global Imagery Browse Services (GIBS) from NASA.

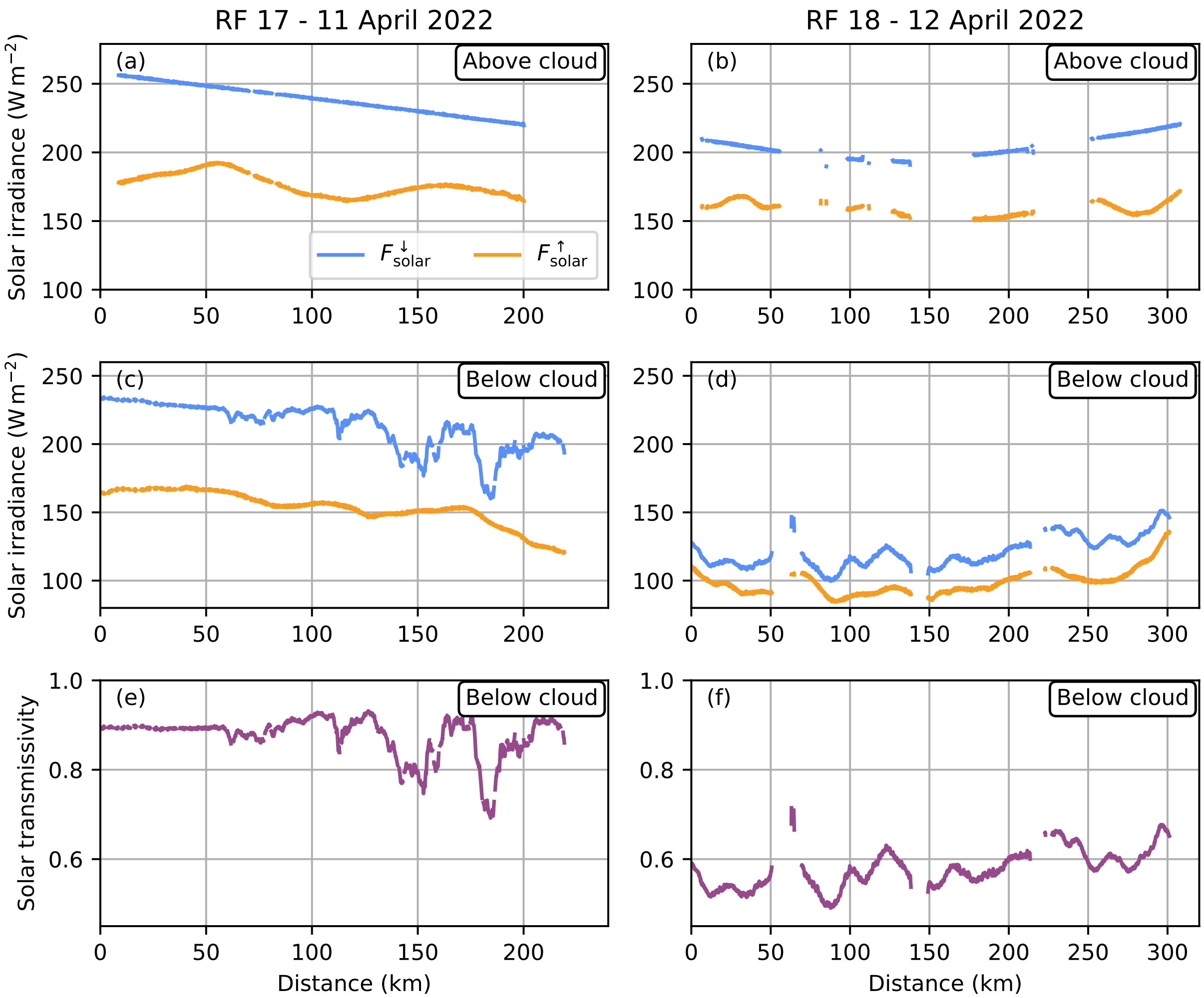

Figure 3: Measured downward and upward solar irradiance from BACARDI for the (a, b) above and (c, d) below-cloud sections of (a, c) RF 17 and (b, d) RF 18. Panels (e) and (f) show the solar transmissivity below cloud. The x-axis shows the distance traveled by HALO from the start to the end of the above-cloud section.

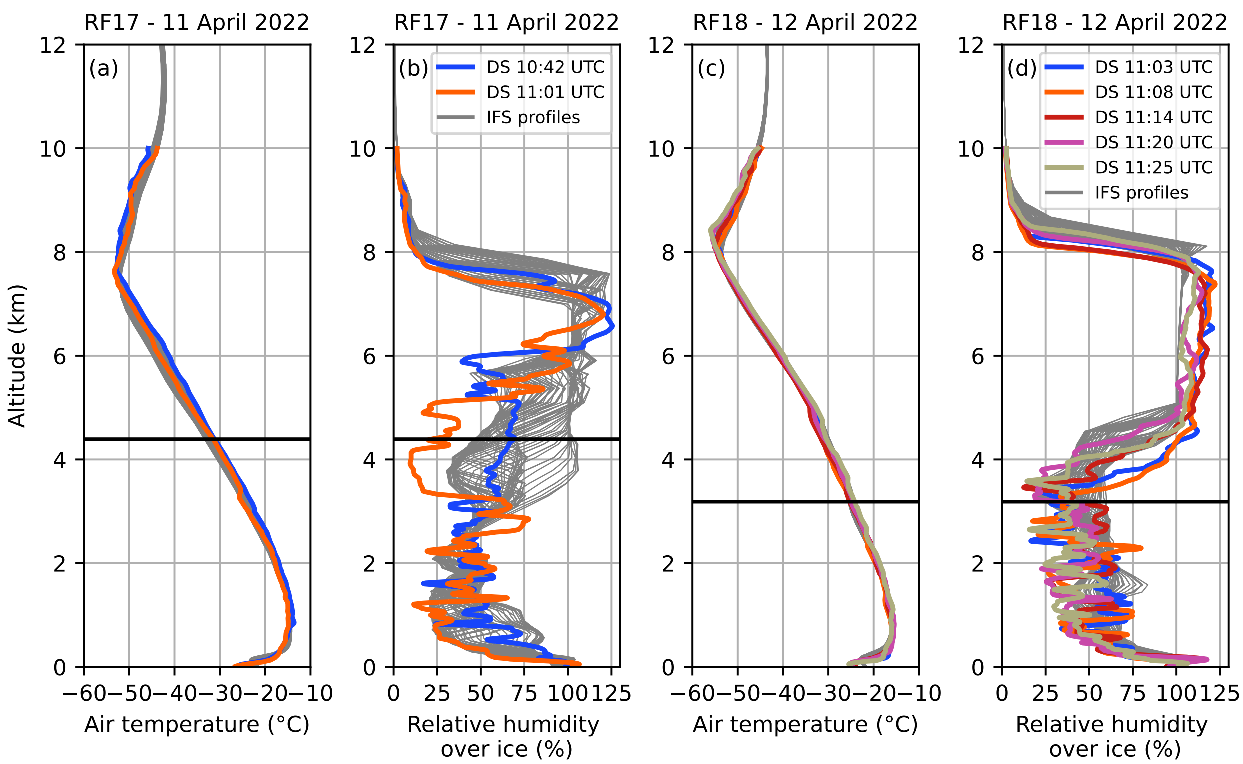

Figure 4: Atmospheric profiles of (a, c) air temperature and (b, d) relative humidity over ice from the IFS (grey lines) for the whole case study period (above and below-cloud section) along the flight track and the dropsondes (DS) deployed by HALO during the above-cloud section of (a, b) RF 17 and (c, d) RF 18. The black line indicates the flight altitude of HALO during the below-cloud section.

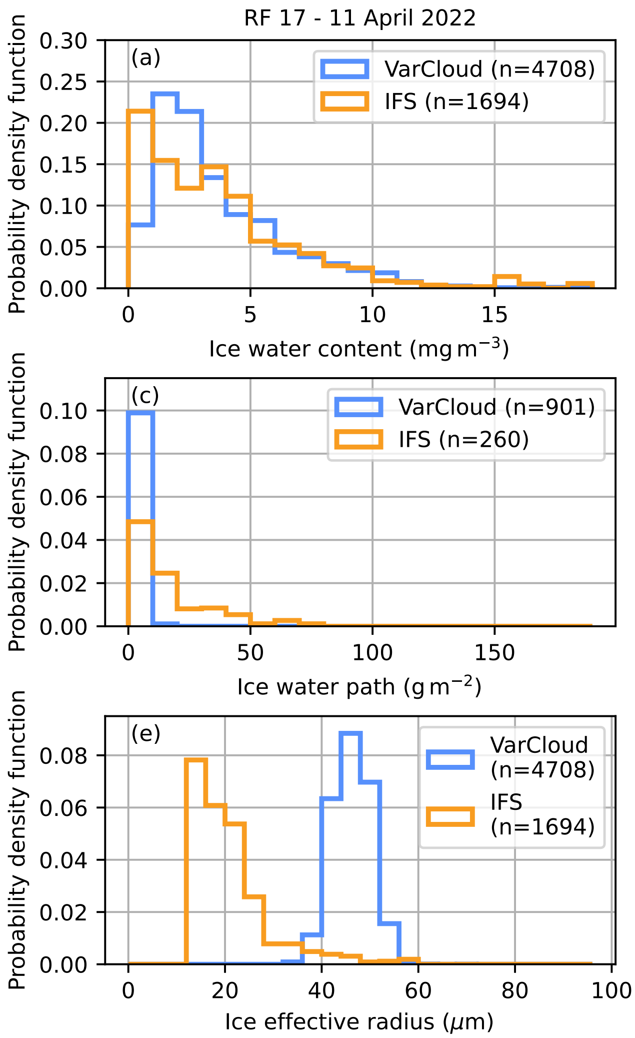

Figure 9: Probability density functions of (a, b) IWC with $1\,\mathrm{mg\,m^{-3}}$ binwidth, (c, d) IWP with $10\,\mathrm{g\,m^{-2}}$ binwidth and (e, f) r_{eff} with $4\,\mathrm{\mu m}$ binwidth for (a, c, e) RF 17 and (b, d, f) RF 18 of the IFS/parameterization output from the below-cloud section and the VarCloud retrieval. n depicts the number of points used in each histogram.

References

Baran, Anthony J., Peter Hill, David Walters, Steven C. Hardiman, Kalli Furtado, Paul R. Field, and James Manners. 2016. "The Impact of Two Coupled Cirrus Microphysics–radiation Parameterizations on the Temperature and Specific Humidity Biases in the Tropical Tropopause Layer in a Climate Model." *J Climate* 29 (14): 52995316. https://doi.org/10.1175/jcli-d-15-0821.1.

Ewald, Florian, Silke Groß, Martin Wirth, Julien Delanoë, Stuart Fox, and Bernhard Mayer. 2021. "Why We Need Radar, Lidar, and Solar Radiance Observations to Constrain Ice Cloud Microphysics." *Atmospheric Measurement Techniques* 14 (7): 5029–47. https://doi.org/10.5194/amt-14-5029-2021.

Foot, J. S. 1988. "Some Observations of the Optical Properties of Clouds. II: Cirrus." *Quart. J. Roy. Meteorol. Soc.* 114 (479): 145164. https://doi.org/10.1002/qj.49711447908.

Fu, Qiang. 1996. "An Accurate Parameterization of the Solar Radiative Properties of Cirrus Clouds for Climate Models." *J Climate* 9 (9): 20582082. https://doi.org/10.1175/1520-0442(1996)009%3C2058:aapots%3E2.0.co;2.

Hogan, Robin J., and Alessio Bozzo. 2018. "A Flexible and Efficient Radiation Scheme for the ECMWF Model." *J. Adv. Model. Earth Syst.* 10 (8): 19902008. https://doi.org/10.1029/2018ms001364.

Hogan, Robin J., Lin Tian, Philip R. A. Brown, Christopher D. Westbrook, Andrew J. Heymsfield, and Jon D. Eastment. 2012. "Radar Scattering from Ice Aggregates Using the Horizontally Aligned Oblate Spheroid Approximation." *Journal of Applied Meteorology and Climatology* 51 (3): 655–71. https://doi.org/10.1175/JAMC-D-11-074.1.

Sun, Zhian. 2001. "Reply to Comments by Greg m. McFarquhar on 'Parametrization of Effective Sizes of Cirrus-Cloud Particles and Its Verification Against Observations.' (October b, 1999,125, 3037–3055)." *Quart. J. Roy. Meteorol. Soc.* 127 (571): 267271. https://doi.org/10.1002/qj.49712757116.

Sun, Zhian, and Lawrie Rikus. 1999. "Parametrization of Effective Sizes of Cirrus-Cloud Particles and Its Verification Against Observations." *Quart. J. Roy. Meteorol. Soc.* 125 (560): 30373055. https://doi.org/10.1002/qj.49712556012.

Yi, Bingqi, Ping Yang, Bryan A. Baum, Tristan L'Ecuyer, Lazaros Oreopoulos, Eli J. Mlawer, Andrew J. Heymsfield, and Kuo-Nan Liou. 2013. "Influence of Ice Particle Surface Roughening on the Global Cloud Radiative Effect." *Journal of the Atmospheric Sciences* 70 (9): 2794–2807. https://doi.org/10.1175/JAS-D-13-020.1.